EE3L11: Bachelor Thesis

Nuna Car Sensor-system - Current sensor

Bachelor graduation project

TSING SHEK - 4401670
JOHAN VLIEGENTHART - 4409256

DELFT UNIVERSITY OF TECHNOLOGY

FACULTY OF ELECTRICAL ENGINEERING, MATHEMATICS
AND COMPUTER SCIENCE

ELECTRICAL ENGINEERING PROGRAMME

August 3, 2018

Abstract

The aim of this thesis is to design a high precision current sensor for the Nuna solar car. A shunt based current sensor was chosen and a circuit is designed based on this method. In order to improve the accuracy a temperature compensation is needed.

Preface

This thesis is written in on behalf of the Nuon Solar Team. We were very excited to participate in such a successful team. We would like to thank Casper van Wezel for giving us this opportunity. A special thanks goes to our supervisor Ir. Dr. C.J.M. (Chris) Verhoeven who supported us and provided us with feedback during the project.

Contents

1 Introduction

Every year, the Nuon Solar Team builds a new solar powered car. The team consists of ten students, which hail from all different faculties at the Delft University of Technology. The car competes at the absolute top of its class and has won almost all World Solar Challenges in Australia and South Africa since 2001 [1]. Needlessly to say, the team is driven to be the best and continuously looking to improve the performance of their car, Nuna.

The ability to monitor the behaviour of Nuna helps to make strategic decisions during the race and could uncover where more performance enhancements are possible. However this would require sensors around and in the car to collect this data. Since the team itself is working with limited time, such large projects are difficult to pursue, especially with required background knowledge on electronics, microcontrollers and software. Due to the these limitations, this project has been outsourced as a bachelor graduation project electrical engineering.

1.1 Group assignment

The task of this bachelor group is to make a sensor system that monitors different aspects of the car. Two sensors have to be designed during the project and a microcontroller to process the measured data. The main priority is to develop a current and voltage sensor that will replace the sensor currently used in the car. The group is split into three subgroups, each with a different task.

The first subgroup will develop a microcontroller that can process the output of the sensors and communicate with the board computer of Nuna. The microcontroller must be designed in such a way that it very easy to connect extra sensors in the future.

The second subgroup focuses on the current and voltage sensor. The main challenge is to measure the current precisely. With the measured data the main computer can monitor the power flows in the subsystems in Nuna and calculate the energy level of the battery.

The third subgroup has the task of making a tire wear sensor. The sensor must be able to monitor the condition of the tires and predict when it needs to be replaced. Secondary this subgroup will assist the second subgroup in the development of the current sensor.

Figure 1 gives an overview of the aspects in the sensor system.

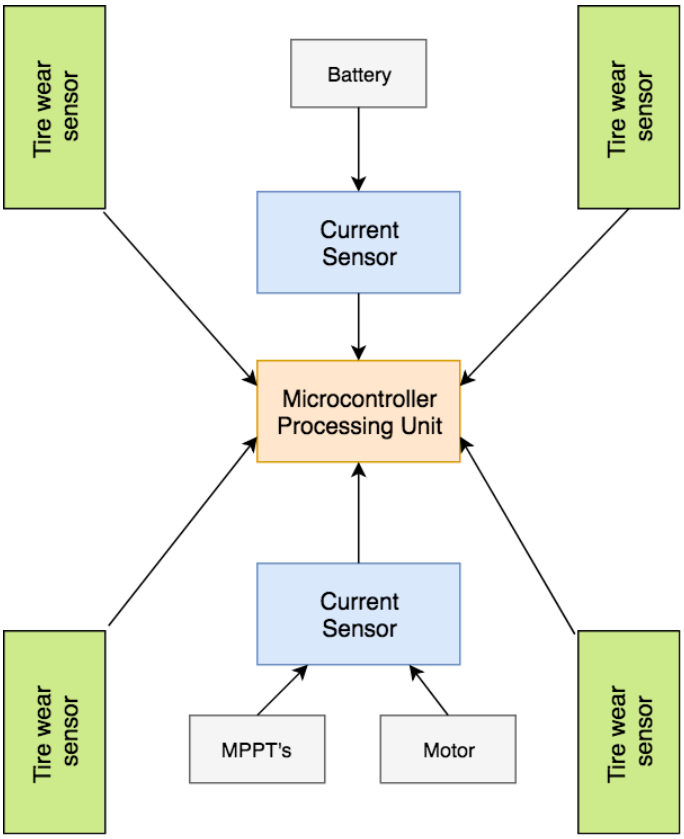

Figure 1: Sensor system

1.2 'State of the art' Analysis

The electrical network of Nuna consist of a high power ($\sim 150V$) and a low power ($12V$) grid, see figure 2. The high power grid is the main focus of this report. The high power network consists of the battery, the electrical motor and the solar panels. Note: The solar panels are controlled by Maximum power point trackers (MPPT), in the remaining of the report MPPT is used as a reference to the combined output of the solar panels.

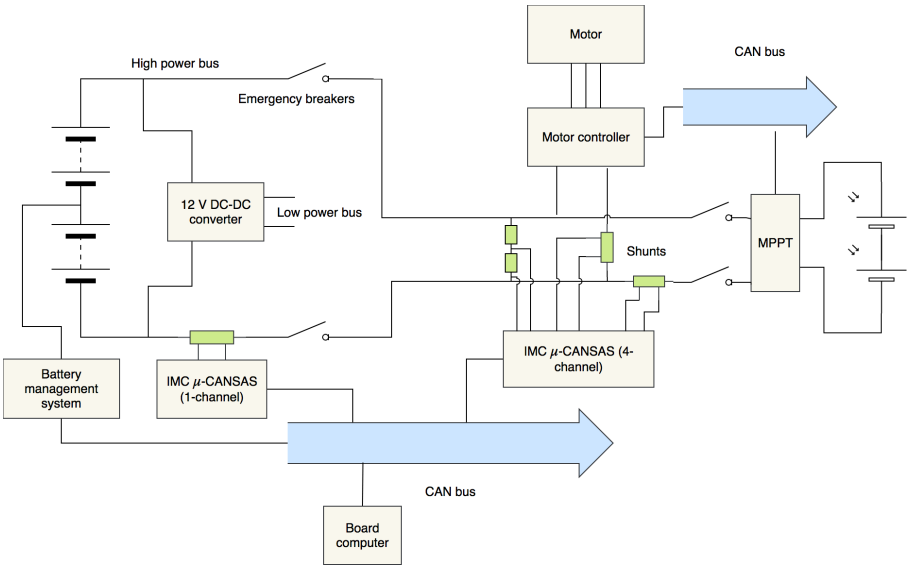

Figure 2: Electrical network of Nuna

Currently the voltage and the current in the high power network are measured by the μ-CANSAS, a product of the company imc. The current is measured at three positions, namely at the output of the motor, the output of the MPPT and low side of the battery.

The currents at the different positions have different characteristics. The motor can consume or produce power, the battery can supply power or charge itself and the MPPT can as well supply power to the battery as to the motor. Figure 3 and table 1 show the statistics of the currents measured in Nuna during the World Solar Challenge 2017.

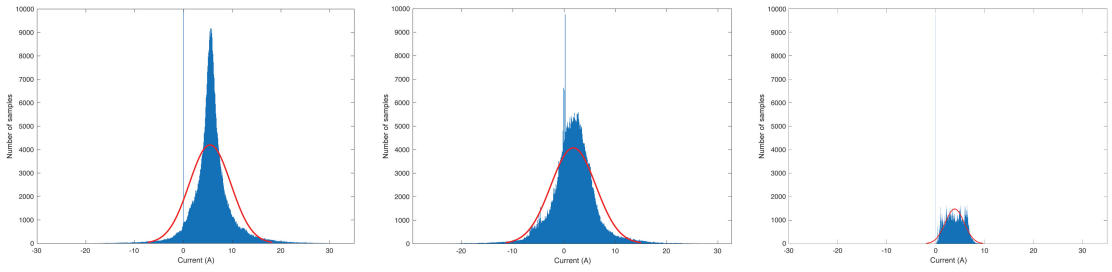

Figure 3: Current distribution of the motor, battery and MPPT sensors measured during World Solar Challenge 2017

Position	Minimum	Maximum	Average	Average absolute value
Motor	-27.19A	34.06A	5.91A	6.65A
Battery	-29.43A	32.54A	1.83A	3.54A
MPPT	0.10A	9.78A	3.96A	3.96A

Table 1: Statistic of the measured currents during World Solar Challenge 2017

1.3 Problem definition

The power flow in Nuna and the energy left in the battery has to be monitored. In order to monitor the power flow in the car the current must be measured at three different positions, namely at the battery, the motor and the MPPT, see figure 2. The voltage must be measured between the plus and the minus of the battery.

1.4 Report overview

In section 2 the requirements for the system will be outlined. Section 3 explains the design and the choices made for each part of the sensor. The test setup and results are shown in section 4. Section 5 explains the compensation of the circuit. Section 6 will discuss the result followed by the conclusion of the report in section 6.

2 Programme of Requirements

The programme of requirements is formulated based on the problem definition and in collaboration with our client Nuna. The choices made in developing the product will be based on the following requirements.

Mandatory requirements

This group of requirements concerns the features which determine if the product delivered is a success. These requirements must be achieved and can never be compromised.

[1.1] The sensor must be able to measure the direct current (DC) flows in the car in a range of -50A to 50A.
[1.2] The sensor must be able to measure the DC current with a precision of at least 2.5mA.
[1.3] The sensor must operate according to the requirements in a temperature range of 0°C to 60°C.
[1.4] The measurements have to be communicated five times a second with the board computer of Nuna.
[1.5] The output signal of the sensor must be between 0V and 5V and must have frequency lower than 1 kHz.

Trade-off requirements

This section contains the features which would make the client increasingly satisfied if the requirements are met.

[2.1] The sensor should preferably be able to measure the DC current with a precision of 1mA.
[2.2] The sensor should be optimized to minimize the power consumption.

3 Design Overview

3.1 Different current sense methods

- Shunt resistor sensor
- Copper trace sensor
- Hall effect sensor
- Magneto resistance effect sensor
- Fluxgate sensor
- Fiber optic current sensor

3.1.1 Ohm's law of resistance

$$V = I * R \tag{1}$$

Equation 1 represents Ohm's law. By measuring a voltage drop over a known resistance the current can be calculated.

Shunt resistor sensor

A Shunt resistor sensor measures the voltage drop over a low resistance. Using the voltage drop and equation 1 the current can be calculated. The shunt resistor sensor is simple to implement and reasonable accurate. However, the shunt resistor has a lack of electrical isolation. The resistor is placed in the current loop and therefore dissipates power from the circuit squared with the current ($I^2 * R$) [2]. In high current systems this will result in substantial losses.

Shunt resistors can exhibit thermal drift, but are built with materials that have low values for the temperature coefficient of resistance ($< 20ppm/K$). The high temperature coefficient of the contact resistance between the shunt resistor and its location can result in substantial errors, because it affects the total amount of thermal drift in the entire device. This can however be solved with the 'four-wire Kelvin principle'.
A resistor exhibits thermal noise regardless of an applied voltage or not. The thermal noise spectral density can be expressed as:

$$N = 4 * k * T * R \tag{2}$$

with N = Spectral noise density [V^2/Hz], k = Boltzmann's constant [J/K], T = Temperature [K], R = Resistance [Ω].
Since the shunt resistor measures a DC current, the thermal noise becomes white noise. Because the differential amplifier connected to the shunt resistor performs an integration, the white noise will have no influence since it stays constant.

Copper trace sensor

This technique utilizes the copper wiring on a PCB. The sensor measures the voltage drop over the copper [3]. The advantage is that it does not require an additional resistance and therefore does not dissipate any additional power. But has also some obstacles:

- Thermal drift of copper. The temperature coefficient of resistance for copper is 3930ppm/K.
- The resistance value cannot be determined very precise before fabricating because of the tolerance in the cross-sectional area and length in the production process.

- Skin effect, the current density is increases at the surface for alternating current and so the resistance changes based on the position.
- Seebeck effect, conversion of heat into electrical current at the junction of two different materials because of a temperature difference.

It is possible to overcome these obstacles [3]. However this technique is not suitable for Nuna because the current has to be measured in different cables and not on a PCB.

3.1.2 Faraday's law of induction

There are a few different techniques based on Faraday's law of induction. Examples are a current transformer and a Rogowski coil. However, sensors based on the Faraday's law sense an alternating current (AC) and the car is powered on direct current (DC). Therefore, this class of sensors is not further discussed [2].

3.1.3 Magnetic field sensors

Hall effect sensor

Figure 4 shows the basic principle of the Hall Effect. It shows a thin metal plate with current running through the material. When a magnetic field is placed near the plate, a voltage will be generated [4].

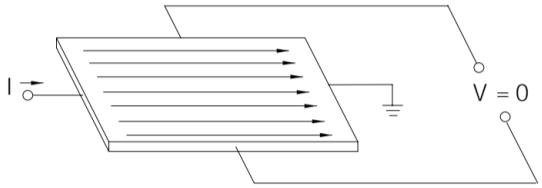

Figure 4: Basic principle of the Hall Effect [4]

An advantage of this technique is that the magnetic field around the conductor is measured. So the sensor does not impact the electrical circuit for a DC current [4] and it does not have power losses squared by the current as the shunt resistor. By using a slotted toroid the Hall effect sensor can be made highly sensitive and immune to external interference. The accuracy for an open-loop sensor is $\pm 1\%$ [5]. To make the sensor even more precise $\pm 0.2\% - 0.5\%$ and fix the linearity and gain errors it is possible to make a feedback loop as shown in figure 5.

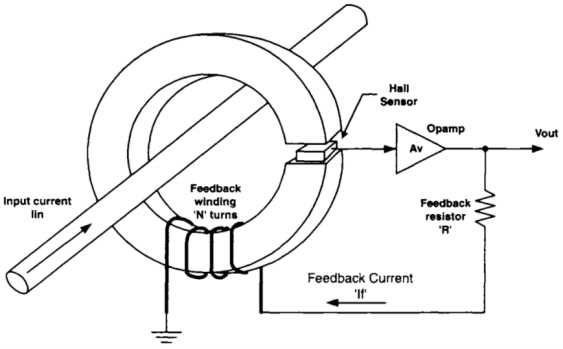

Figure 5: Diagram of a Hall Effect circuit with feedback loop [4]

Magneto Resistance Effect sensors

Unlike the resistors of the sensors based on the Ohm's law, magneto resistance effect sensors make use of resistors, whom resistance changes depending on the applied magnetic field.
The type of magnetoresistor sensor depends on the magnetoresistive elements of the design. Many types of magnetoresistive elements have been developed and the main difference between the elements are their sensitivity to the magnetic field and the linearity of their response [6].
Although MR sensors have good sensitivity and accuracy and provides electrical insulation, they typically suffer from high thermal drift and non-linearity. This issue can be solved with a closed loop configuration, but this comes with adding cost to the overall design. Also, MR sensors are very susceptible to external magnetic fields and can even become useless when exposed to a strong magnetic field [2].

Fluxgate sensor

Fluxgate sensors exploits magnetic induction and the saturation of ferromagnetic materials at high fields. When a large enough AC current is applied to the drive coil, the magnetic core reaches its saturation every half-cycle. During the saturation, the magnetic flux remains the same, even when the magnetic field increases. Therefore, the core is less sensitive to external magnetic field during saturation. On the other hand, when the core is not saturated, it is sensitive to external magnetic fields.
When the external magnetic field is 0, the input and the output current matches. However, when the external magnetic field has nonzero value, the core becomes more or less easily saturated. This all can be detected in the secondary coil, which is called the sensing coil [7].
Due to their high sensitivity and temperature stability of the fluxgate sensors, they are most accurate magnetic field sensors available. However, these devices tend to be bulky and not as rugged as other technologies [8].
Figure 6 shows the principle behind fluxgate sensors.

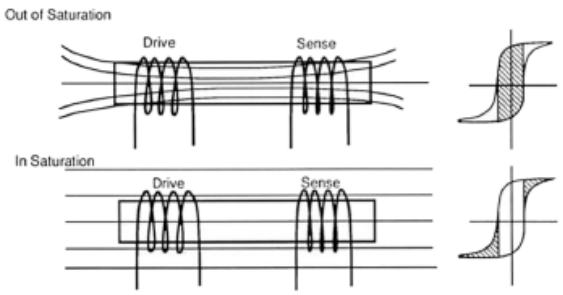

Figure 6: The magnetic field during saturation and out of saturation [7]

3.1.4 Faraday Effect

The Faraday Effect describes the interaction between light and a magnetic field in a medium. When light travels through a medium in a magnetic field, its polarization vector rotates proportionally to the magnetic field vector. The following equation describes the relationship between the magnetic field and the plane of polarization of a linearly polarized light [9]:

$$\phi = V \int \vec{B} \cdot dl \tag{3}$$

where V is the Verdet constant, it describes the strength of the Faraday effect in a certain medium in which the light travels and B is the applied magnetic field. Since B is proportional to the current, ϕ is also proportional to the current.

Fiber optic current sensor

The Faraday Effect-based current sensors are called fiber optic current sensors, because the sensors use optical fiber as a medium to transmit the light. Fiber optic current sensors have many advantages [10], such as:

- Immunity to external electromagnetic fields,
- Electrically isolated,
- High sensitivity,
- Compact and light weight.

Due to the high sensitivity of this type of sensor, they are highly sensitive to external factors such as bending, vibration and the temperature [10], which cause a reduction of the accuracy of the sensor. As a result of this, compensation is needed to deal with these issues and the overall cost and complexity of such sensors are relatively high compared to the alternatives mentioned. Currently, they are only commercially used for high current applications. Since a failure in such a system causes huge losses and therefore the high cost of the sensors are justified. Moreover, the noise of the system and the received optical signal deteriorate the response of the sensor at lower current amplitudes, thus decreasing the accuracy as the current decreases [9]. As of now, a fiber optic current sensor for low DC currents with an accuracy comparable to the current sensor of the Nuna remains yet to be found.

Sensor	Accuracy	Power loss	Suitable
Shunt resistor	0.1% - 2%	mW - W	Yes
Copper trace	0.5% - 5%	mW	No
Hall effect	0.2% - 2%	mW	Yes
MR	0.5% - 2%	mW	Yes
Fluxgate	0.001% - 0.5%	mW - W	Yes
Fiber optic	0.1% - 1%	W	No

Table 2: Comparison between the different sensors [2, 5, 10]

3.1.5 Shunt vs Hall

Finally, an overview has been made for final comparison between all the sensors above in table 2. Based on table 2, the shunt resistor current sensor, the hall effect current sensor, the magneto resistance effect current sensor and the fluxgate current sensor are the ones that are suitable for measuring DC current in the Nuna. After a market research, it turned out that the magneto resistance current sensor and the fluxgate current sensor were not readily available or only available in bulk. Therefore, the shunt resistor current sensor and the hall effect current sensor could only be tested for a comparative analysis.
The shunt resistor current sensor and the hall effect current sensor have been analyzed over a current range of -30A to 30A. The range of -50A to 50A could not be measured, because 30A was the maximum current of the equipment that was available to the group.
The plot of the measured output voltage, expected output voltage and the error percentage is illustrated in figure 7 for the shunt and figure 8 for the hall. As can be seen in the 2 figures, the error percentages of the shunt resistor current sensor is slightly lower, but since the differences are so small, it remains inconclusive which sensor is better.

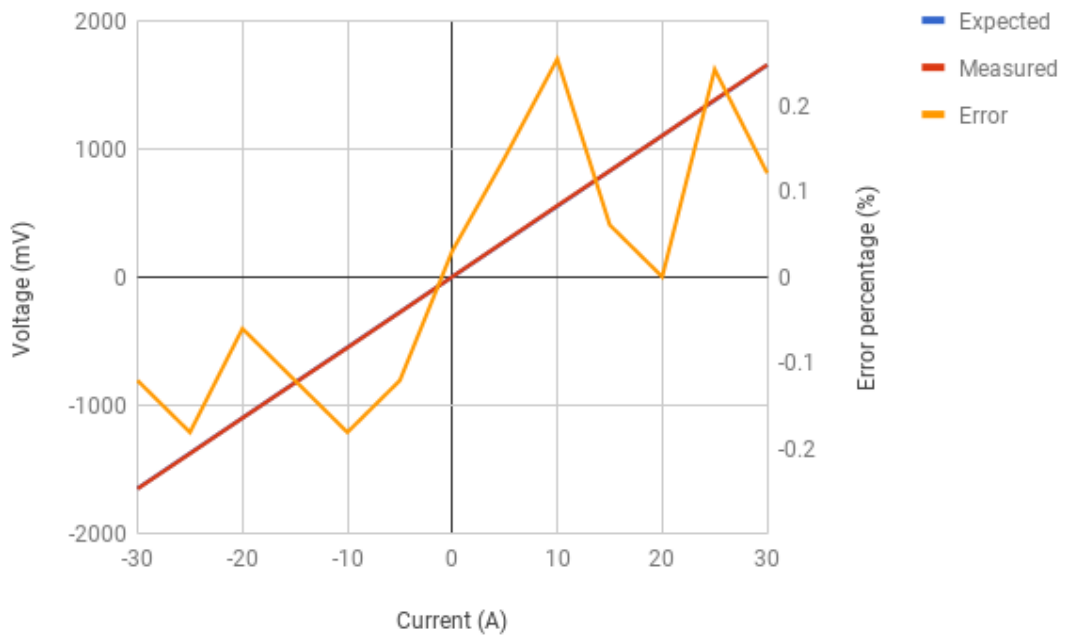

Figure 7: The output voltage and error of the shunt resistor current sensor over a current range of -30A to 30A

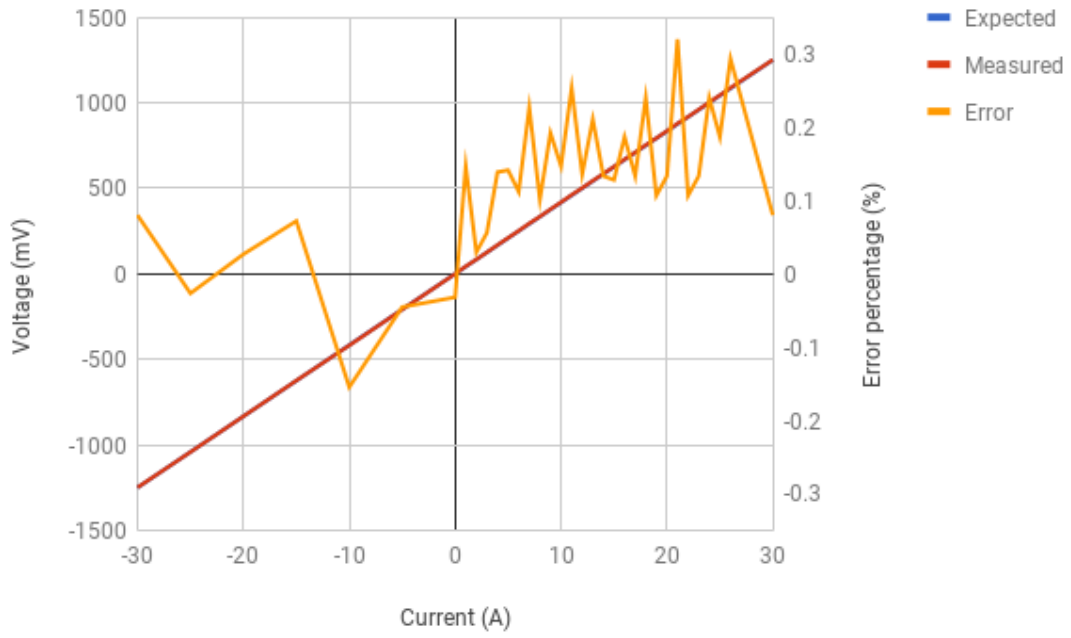

Figure 8: The output voltage and error of the hall effect current sensor over a current range of -30A to 30A

Both sensors were also tested on their temperature dependence, the shunt was tested over a range of $-20°C$ to $60°C$ and the hall was tested over a temperature range of $0°C$ to $55°C$. The plots of the offset voltage of

both sensors are illustrated in figure 9 and 10. The hall effect current sensor has a much higher temperature dependence than the shunt resistor current sensor.

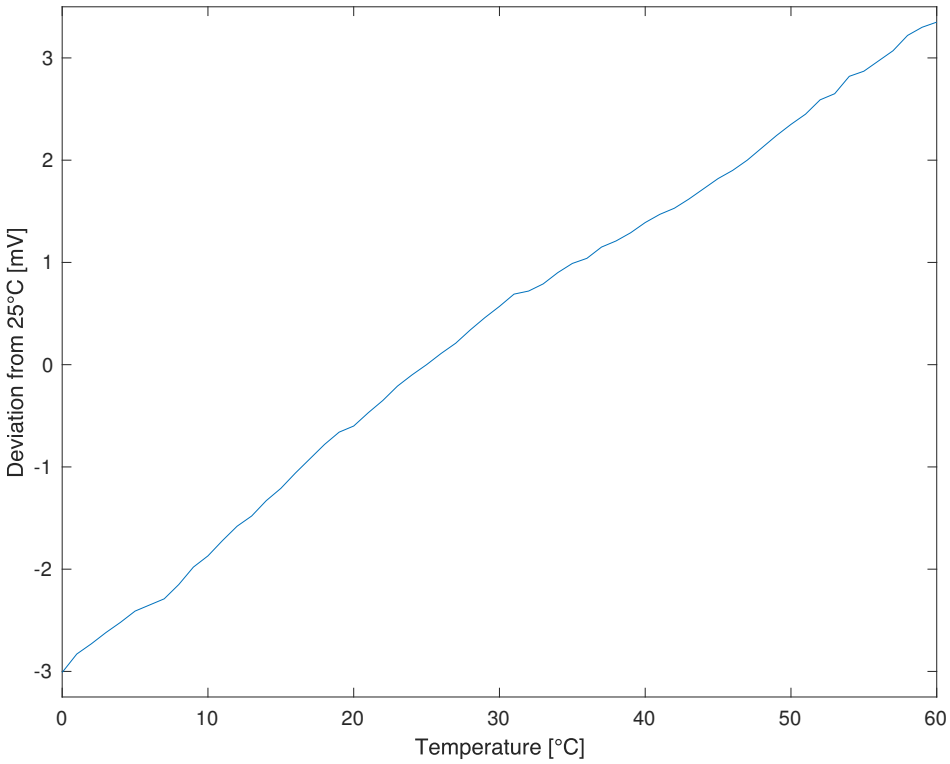

Figure 9: The offset of the shunt resistor current sensor over a temperature range of 0°C to 60°C

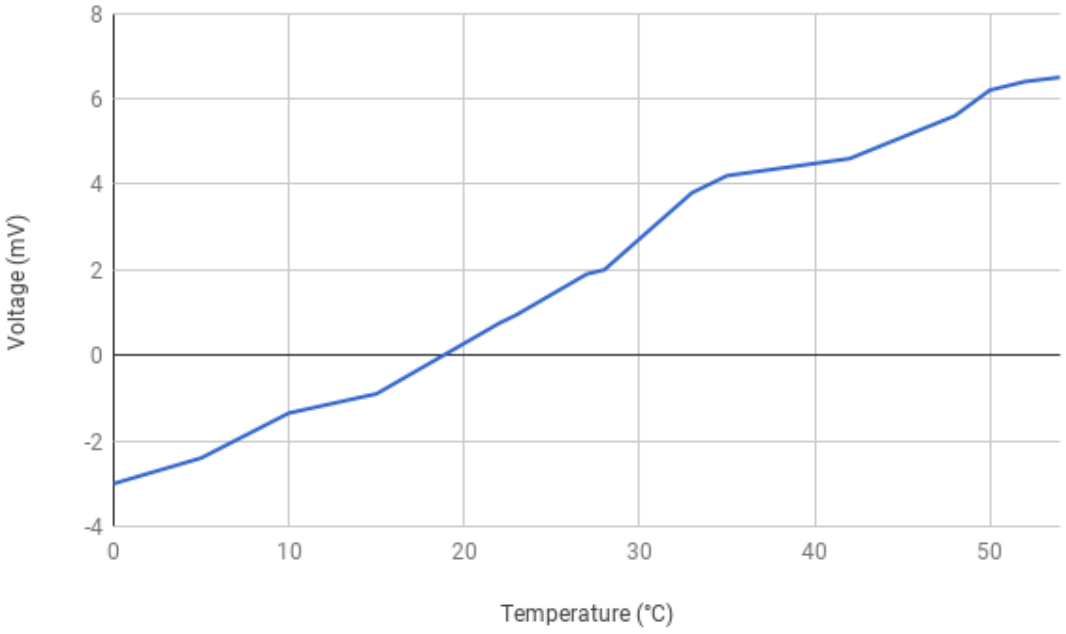

Figure 10: The offset of the hall effect current sensor over a temperature range of 0°C to 55°C

Even though the accuracy of the two sensors are comparable over a constant temperature, the hall sensor has a much higher temperature drift than the shunt current sensor. Therefore, the shunt resistor current sensor has been chosen and this sensor type will be further investigated in the upcoming chapters.

3.2 Functional overview

In order to design the sensor efficiently, the sensor is divided into different elements. Figure 11 illustrates the subsystems in the sensor.

The system will contain the following elements:

- Shunt resistor
- Filter
- Bias
- Amplifier

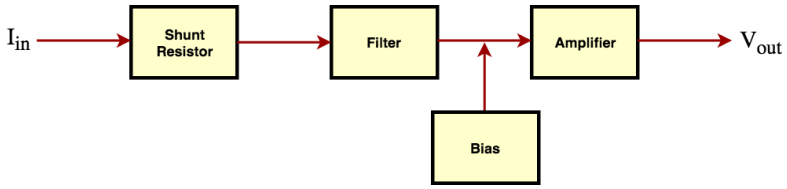

Figure 11: Functional overview of the sensor

The shunt resistor is essentially a current-to-voltage converter in this system. The current that goes through the shunt resistor results in a voltage across it.
To limited the noise the signal is filtered with a low-pass filter.
The system needs to be able to measure bidirectional current, therefore the input signal of the amplifier needs to be biased.
At last, the system needs to have an output with a range of 0 - 5 V which is mapped from the current range of -50 A to 50 A. Since the shunt resistor has a small resistance, a small voltage will be created. Therefore, an amplifier is needed to amplify this small voltage signal to an useful amplitude.

3.3 Output signal

The Programme of Requirements, section 2, states that the sensor should preferable be able to reach an accuracy of 1 mA in a range of -50 A to 50 A with an output signal between 0V and 5V (requirements [1.1], [1.5] and [2.1]). This means that every input step of 1mA corresponds with $5V/(100A * 10^3) = 50\mu V$ at the output.

The output will be processed by the ADC developed by the microcontroller subgroup. To be able to reach an accuracy of 1 mA, the lowest significant bit of the ADC should be lower than or equal to $50\mu V$. With the full range being 5V, there should be at least $5V/50\mu V = 100,000$ steps. Equation 4 shows that the ADC needs to have a resolution of 17 bits or higher.

$$2^N \geq 100,000 \implies N \geq \log_2 100,000 \approx 16.6 \qquad \text{N = number of bits} \tag{4}$$

In order for the ADC to recover the $50\mu V$ signal, the signal-to-noise ratio (SNR) of the output of the sensor should be at least 6.02 * 17 bits + 1.76 = 104.1dB [11]. The maximum noise level in the signal therefore should not exceed $5V * 10^{104.1/20} = 31.2\mu V_{p-p}$.

3.4 Noise

Noise can be seen as random fluctuations of current or voltage in an electrical circuit. Noise is a very important aspect in designing an accurate sensor system. Therefore, for every component it will be analyzed. Moreover, the signal-to-noise ratio determines the resolution of an ADC. If the signal-to-noise ratio is not high enough, the lowest bits of the ADC will be fluctuating constantly and are useless to a sensor system. The signal power has to be increased or the noise power has to be decreased, to be able to increase the signal-to-noise ratio. The signal power can only be increased up to certain point, since the electrical power is a limiting factor. Therefore, reducing the noise power is the only option.
There are three different types of noise that are relevant in an amplifier circuit:

- Thermal noise
- Flicker noise
- Shot noise

3.4.1 Thermal noise

Thermal noise is generated by random movements of charges, caused by thermal agitation, in a conductor. Thermal noise has a flat spectral density, therefore it is independent of the frequency and can be considered as white noise [12]. The thermal noise voltage in rms of a resistor is the following [12]:

$$e = \sqrt{4kTR \times ENB} \tag{5}$$

k is Boltzmann's constant ($1.38 \times 10^{-23} J/K$),
T is temperature in Kelvin (K),
R is resistance of the resistor in ohm (Ω) and
ENB is the equivalent noise bandwidth in Hertz (Hz).
A resistor with thermal noise can be modeled as a voltage source in series with a noiseless resistor.

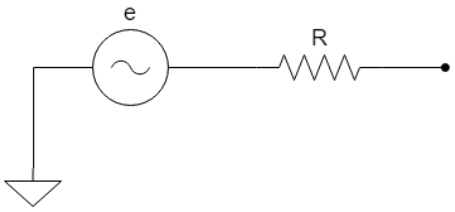

Figure 12: Resistor with thermal noise

3.4.2 Flicker noise

Flicker noise is also called 1/f noise, because it is the dominant noise at low frequencies (DC). The root source of 1/f noise is still unknown, but it may be related to the imperfections of semiconductors, since better processing reduces this type of noise [12]. The noise mean square voltage of the flicker noise is the following [13]:

$$\overline{e^2} = \int K^2/f df \tag{6}$$

K is device constant that determines the behaviour of the flicker noise,
f is the frequency in Hertz (Hz) and
df is the differential frequency also in Hertz.

3.4.3 Shot noise

In operational amplifiers, shot noise is mainly caused by P-N junction of transistors. Shot noise is a result of charges that cross potential barrier, which results in a burst of current. Like flicker noise, shot noise has a flat spectral density, therefore it is also considered as white noise.

3.4.4 Multiple noise sources

There are different types of noise mentioned in sections above. All of the noise sources need to be combined to get a useful noise analysis of the whole system. However, the equivalent noise source can be calculated by the following equation [12]:

$$E_N = \sqrt{E_1^2 + E_2^2 + \ldots + E_{n-1}^2 + E_n^2} \tag{7}$$

3.5 Shunt resistor

The first element of the sensor is the shunt resistor. The resistor will be placed in the current path that results in a voltage drop across resistor. The resistor can be placed at two positions, before the load (high-side) or after the load (low-side), see figure 13 [14].

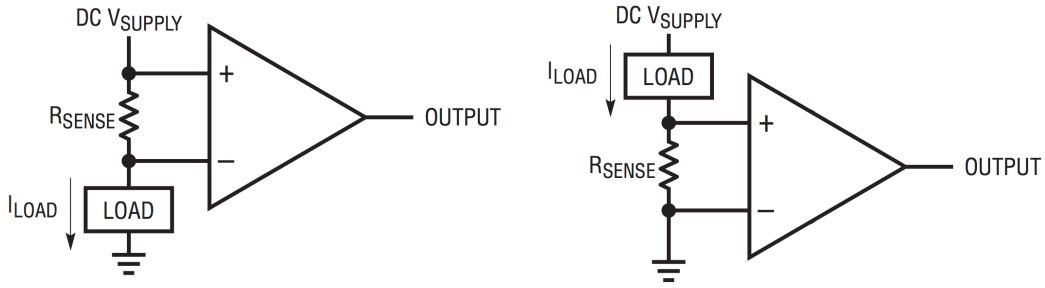

Figure 13: High- and low-side implementation [14]

The main advantage of the high-side implementation is that the load is directly connected to the low side of the battery. The main disadvantage is that the high-side implementation will result in a high common-mode voltage on the input terminals of the amplifier [14]. Due to a possible mismatch between the resistors in the circuit, a common mode error could be introduced [15].

The main advantages of the low-side implementation are the low common-mode voltage on the input of the amplifier and the output of the amplifier that will be referred to the low side of the battery. The disadvantage is the disruption of the connection between load and the low side of the battery [14].

The advantages of the low-side implementation reduce the complexity and eliminate a possible common mode error. Therefore the low-side implementation will be used in the sensor.

An important characteristic of the shunt resistor is the thermal drift [2]. The thermal drift causes an output voltage offset error that can be calculated using equation 8. To minimize the thermal drift a resistor made of a material with a low temperature coefficient (ppm/°C) should be used, like manganese-copper or nickel-chrome alloys.

$$I_{max} * R_{shunt} * Gain * \frac{\text{temperature coefficient}}{10^6} * (\text{max°C} - 25°\text{C})V \tag{8}$$

The shunt resistor is placed directly into the current path of the circuit. This could result in a high power consumption. The power consumption can be calculated the following equation [2]

$$P = I^2 * R_{shunt} \tag{9}$$

In order to reduce the power consumption (requirement [2.2]), the resistance should be as low a possible. The resistor must also be rated to handle 50 A (requirement [1.1]). Keeping both requirements in mind an 1mΩ shunt of Murata Power Solutions is chosen.

The shunt has a temperature coefficient of $\pm$ 15 ppm/°C [16]. According to equation 8, the maximum output offset error with 50A at 60°C (requirement [1.1] and [1.3]) will be 26.25 μV * Gain. The error is too high according to requirement [1.3]. Therefore the temperature behaviour of the shunt should be analyzed and compensated.

There is no noise analysis needed for the shunt resistor, because the shunt resistor will be shorted when using the superposition theorem. Therefore the noise of the shunt resistor has no impact on the output of the system.

3.6 Amplifier

The voltage drop across the shunt resistor will be between -50 mV and +50 mV. So an amplifier is needed to amplify the small voltage to a range between 0 and 5 Volt (requirement [1.5]) and pass the signal on to the ADC.

3.6.1 Gain

The shunt resistor is rated at 50 A and the current sensor should be able to measure bidirectional current, therefore the full range of the current is 100 A, i.e. from -50 A to 50 A. Considering that the shunt resistor is 1 mΩ, the full range of the voltage across the shunt resistor is 100 mV. To make full use of the 5 V range of requirement [1.5], the voltage across the shunt resistor must be amplified by a factor of 50.

3.6.2 Imperfections of the operational amplifier

The operational amplifier has a number of imperfections which can limit the accuracy of the sensor. The most important imperfections are the offset voltage, the temperature coefficient and the input bias current [17].

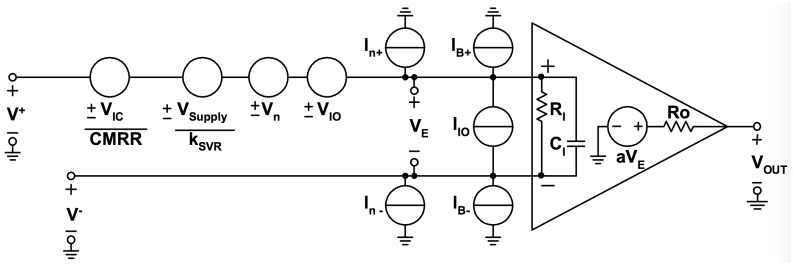

Figure 14: Non-ideal Operational Amplifier Model [18]

Input offset voltage

The input offset voltage (V_{io}) is defined as the voltage that must be applied across the input terminals of the amplifier to result in a zero output voltage. The output is preferably zero when both terminals are grounded. However, a mismatch between the different components and the input transistors inside the amplifier in a voltage drop over the input terminals [18].

Figure 15 shows a simplified model of MOSFET based amplifier. When R1 and R2 are perfectly matched the offset voltage can be calculated with the following equation [19]

$$V_{io} = \frac{V_{GS} - V_T}{2} \frac{\triangle(W/L)}{(W/L)} \tag{10}$$

Where $W/L = \frac{(W/L)_1 + (W/L)_2}{2}$; $\triangle(W/L) = (W/L)_1 - (W/L)_2$.

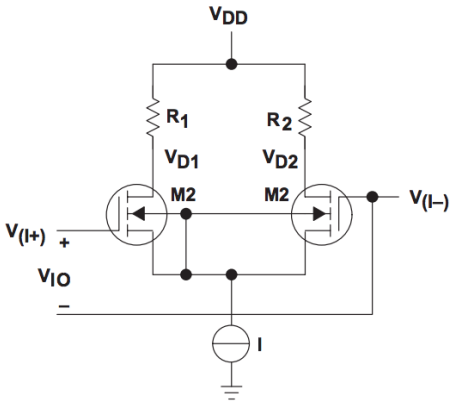

Figure 15: Simplified differential input circuit with MOSFET technology [19]

Temperature coefficient

A closer look at equation 10 shows that the threshold voltage V_T dependents on the temperature [19].

$$V_T = -\frac{kT}{q} ln \frac{N_G N_B}{n_i^2} - \frac{Q_{ox}}{C_{ox}} + 2\phi_F \pm \frac{Q_D}{C_o x} + \gamma(\sqrt{2\phi_F + V_{BS}} - \sqrt{2\phi_F}) \tag{11}$$

So change in temperature will influence the offset voltage of the amplifier . The characteristics of the other components in the amplifier have a temperate dependency as well which is translated in a temperature coefficient.

Input bias current

The input bias current (I_{io}) is defined as the current flowing through the input terminals of the amplifier [17]. In a MOSFET amplifier the bias currents are very small (pA) because it requires very little DC gate current to operate. However bipolar junction transistor amplifiers require base currents for proper bias which result in larger a input bias current (μA) [20].

3.6.3 Differential amplifier topology

A differential amplifier is needed to amplify the the voltage drop across the shunt resistor. Figure 16 shows the topology used to amplify the signal.

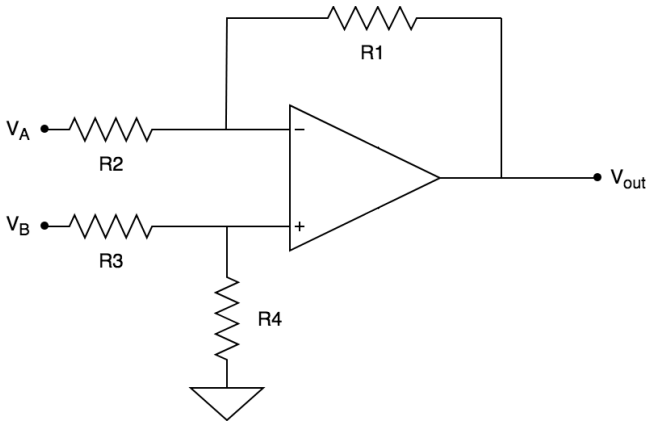

Figure 16: Differential amplifier topology

The output of the amplifier can be calculated using the following equation.

$$V_{out} = \frac{R4}{R3 + R4} * \frac{R1 + R2}{R2} * V_B - \frac{R1}{R2} * V_A \tag{12}$$

With R4 = R1 and R3 = R2 and V_A grounded, because of the low-side implementation, the equation simplifies to

$$V_{out} = \frac{R1}{R2} * V_B \tag{13}$$

The gain is determined by R2/R1. So R1 must be 50*R2 in order to have a gain of 50. R1 and R2 also influence the power consumption of the topology. The power consumption can be calculated using equation 14. In order to minimize the power consumption (requirement [2.2]) R1 + R2 should be as high as possible.

$$P_{feedback} = I_f^2 * (R1 + R2) = \frac{V_{out}^2}{R1 + R2} \tag{14}$$

The error because of the input bias current, see section 3.6.2, can be calculated using the following equation [19]

$$V_{offset} = (I_{B+} * R4) - (I_{B-} * R1) \tag{15}$$

By matching R1 en R4 the voltage offset caused by the input bias current can be eliminated.

3.6.4 Chopper Amplifier

As the voltage offset and the voltage noise are critically important for the uses of the current sensor inside the Nuna, an amplifier with low voltage offset and low voltage noise is needed to reach an accuracy of 2.5 mA or better. These requirements led us to the chopper amplifier as a good solution. The concepts behind the working of the chopper amplifier will be discussed in this part of the chapter.

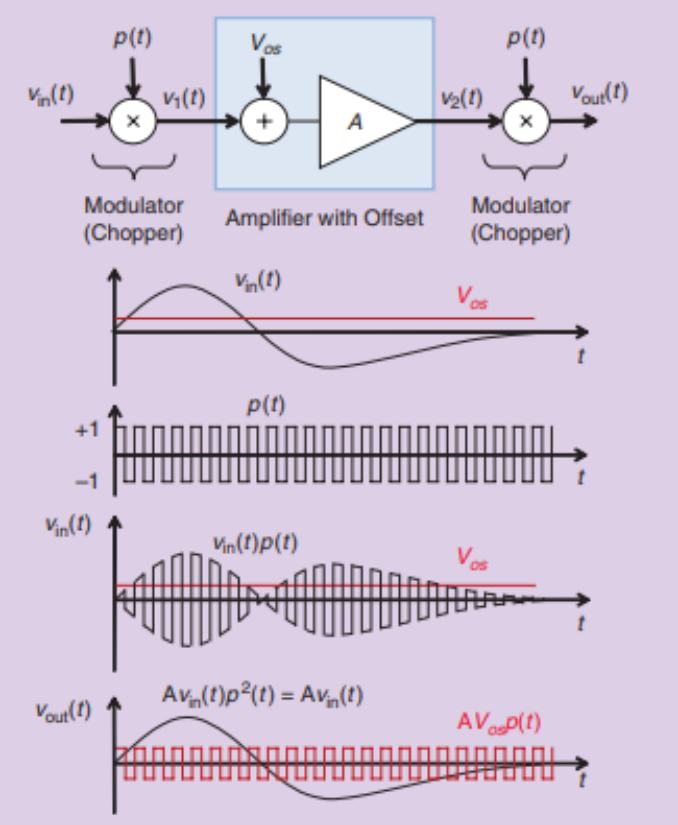

Figure 17: Chopper amplifier [21]

The block diagram with the corresponding waveform of each stage of the chopper amplifier in figure 17 gives a simplified illustration of how the chopper amplifier works.
First, the input signal of the chopper amplifier is modulated to a higher frequency. In this case, this is done by multiplying the input signal with a periodic square wave. As a result, the input signal looks like it has been chopped. Second, the offset voltage of the amplifier is added to the chopped input signal, after which it is amplified by the amplifier, which has a gain of A. Third, this amplified signal is multiplied with a periodic square wave again. Although this time, the original input spectrum is reverted. The offset voltage, however, is modulated to a higher frequency.
The chopped offset voltage can easily be filtered away with a low-pass filter, since the amplified input signal has a spectrum close to DC and the offset voltage has a spectrum near the frequency of the square wave function.
In the same way, the chopper amplifier also eliminates the 1/f noise or flicker noise, which is dominant at low frequency [21].

3.6.5 Noise analysis differential amplifier

There are two types of noise sources in the differential amplifier circuit that are relevant: the thermal noise from the resistors and the 1/f noise and white noise of the operational amplifier. First off, the total thermal noise rms voltage can be calculated by using the superposition theorem and subsequently, adding them with the equation mentioned in chapter 3.4.4.

The superposition theorem isolates each source by shorting each voltage source, therefore the inputs of the differential amplifier are grounded. Figure 18 to 21 illustrates how the superposition theorem is applied to the circuit and equation 16 to 19 show the calculation of the rms noise voltage of each resistor.

$$E_1 = e_1 \frac{R_2}{R_1} \tag{16}$$

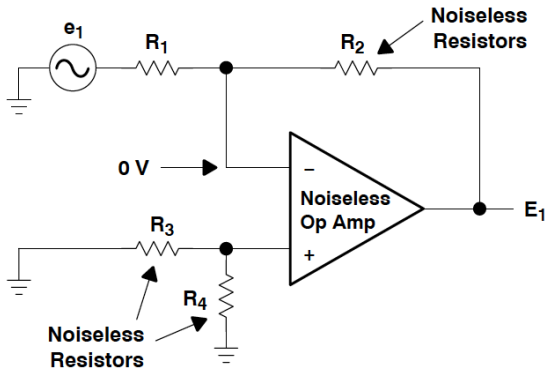

Figure 18: Noise voltage source of R_1 [13]

$$E_2 = e_2 \tag{17}$$

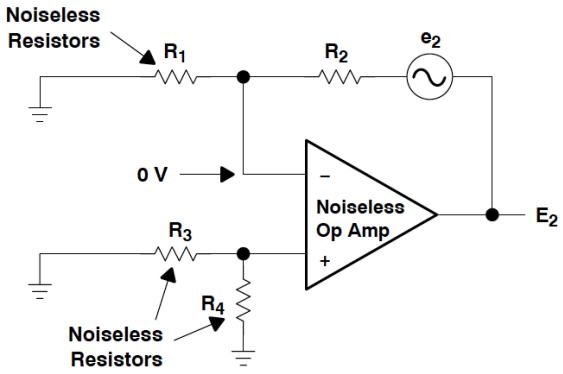

Figure 19: Noise voltage source of R_2 [13]

$$E_3 = e_3 \frac{R_4}{R_3 + R_4} \frac{R_1 + R_2}{R_1} \tag{18}$$

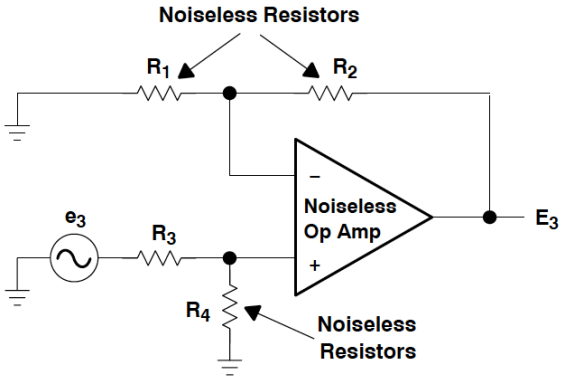

Figure 20: Noise voltage source of R_3 [13]

$$E_4 = e_4 \frac{R_3}{R_3 + R_4} \frac{R_1 + R_2}{R_1} \tag{19}$$

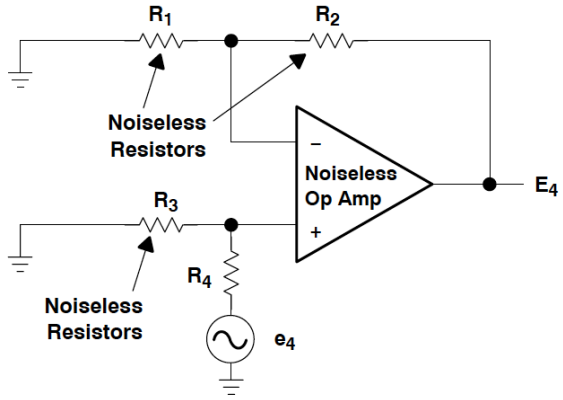

Figure 21: Noise voltage source of R_4 [13]

According to chapter 3.4.1, the thermal noise voltage of each resistor can be calculated as follows:

$$e_n = \sqrt{4kTR_n} \times \sqrt{ENB} \qquad in\, V_{rms} \tag{20}$$

The total thermal noise rms voltage resulted from the resistors of the feedback network can be calculated as follows:

$$E_R = \sqrt{E_1^2 + E_2^2 + E_3^2 + E_4^2} \qquad in\, V_{rms} \tag{21}$$

$$E_R = \sqrt{4kT\left[\frac{R_2^2}{R_1} + R_2 + R_3\left(\frac{R_3}{R_3 + R_4}\frac{R_1 + R_2}{R_1}\right)^2 + R_4\left(\frac{R_3}{R_3 + R_4}\frac{R_1 + R_2}{R_1}\right)^2\right] \times ENB} \tag{22}$$

When $R_1 \approx R_3$ and $R_2 \approx R_4$, equation 22 can be reduced to:

$$E_R \approx \sqrt{8kTR_2\left(\frac{R_2}{R_1} + 1\right) \times ENB} \tag{23}$$

Most data sheets of operational amplifiers describe the noise voltage E_N of a bandwidth from 0.1 Hz to 10 Hz (1/f noise is dominant) in V_{rms} or V_{p-p} and the voltage noise density e_N at 1 kHz (white noise) in $V/\sqrt{Hz}$. Usually there is also a voltage noise density graph.

If the 1/f noise is described in V_{p-p}, it is reasonable to divide it by 6 to get the rms voltage, since most data sheets use peak-to-peak voltage that contains 99.7% of the noise distribution [13].

The white noise rms voltage of the equivalent noise bandwidth from 10 Hz can be calculated as follows:

$$E_w = e_N \times \sqrt{ENB} \tag{24}$$

The total noise rms voltage as a result from the flicker noise and white noise of the operational amplifier is as follows:

$$E_{oa} = \sqrt{E_N^2 + E_w^2} \tag{25}$$

To conclude this, the total noise rms voltage of the differential amplifier is the following:

$$E_{total} = \sqrt{E_R^2 + E_{oa}^2} \tag{26}$$

3.6.6 Component choices

In order to select an amplifier a comparison is made based on the voltage offset, the temperature drift, the voltage noise density and the flicker noise. Figure 22 shows the characteristics of the amplifiers.

Product	Offset (µV)	Drift (µV/C)	Noise (nV/√Hz)	1/f (µVpp)	Drift @ +25C * Gain (50) [µV]
OPAx189	3	0.02	5.2	0.1	25
OPAx388	5	0.05	7	0.14	62.5
OPAx211	124	1.5	2	0.08	1875
OPA1212x	500	4	2	1.2	5000
OPAx209	150	3	3.3	0.13	3750
MAX44250	9	0.026	6.2	0.123	32.5
MAX44251/2	6	0.019	6.2	0.123	23.75
MAX4424x	5	0.02	9	0.117	25
MAX4238	2	0.01	30	1.5	12.5

Figure 22: Amplifier comparison

Based on the comparison in figure 22 the OPAx189 developed by Texas Instruments and the MAX44251/2 developed by Maxim Integrated are selected for further testing.

The orange curve in figure 23 shows the relation between the power consumption and the value of R1 in the feedback loop (equation 14). The blue curves represent the thermal noise based on the value of R1 for different equivalent noise bandwidths (equation 23).

In order to reduces the power consumption (requirement [2.2]) the value of R1 should be as high possible. However a high R1 will introduce a lot of noise and lower the accuracy (requirement [1.1] and [2.1]). The filter, see section 3.8, requires a high resistor as well. As a compromise a resistance of 25 kΩ will be used for R1. Therefore R1 and R4 will be 25 kΩ and R3 and R2 will be 500 Ω.

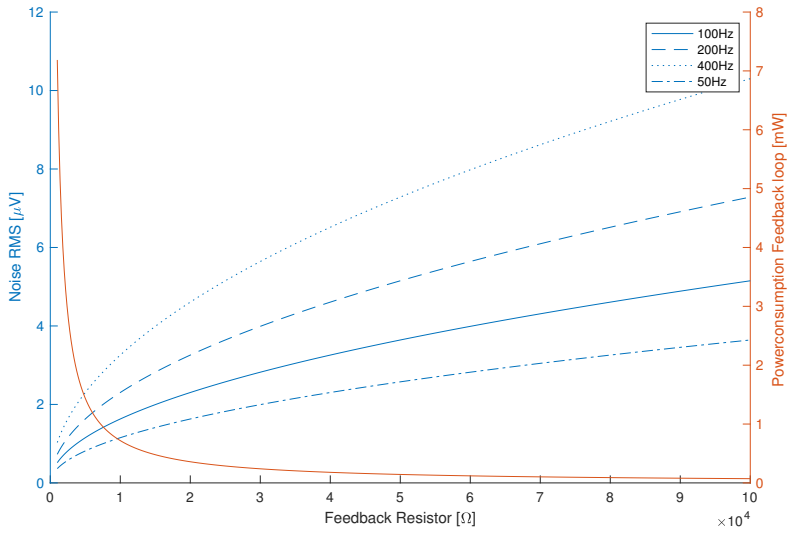

Figure 23: Thermal noise and power consumption versus R1 resistance value

3.7 Biasing

To fulfill requirement [1.1], the current sensor needs to be able to measure negative currents as well. A negative current through the shunt resistor creates a negative voltage across it. To be able to get a useful value at the output of the operational amplifier, the operational amplifier needs either to be able to handle a negative supply in addition to a positive supply or the amplifier circuit needs to be biased to a high enough voltage to be able the cover the range mentioned in requirement [1.1]. The latter is chosen, since an extra voltage regulators will be needed for the first option, while with the latter option less power consuming circuits can be used. These circuits are called voltage references and they provide a much more stable voltage than regulators in general [22].

Currently, there are two voltage references topologies available on the market: series and shunt. Inherently, there are no differences in accuracy between the two. The main advantage a series voltage reference has over its counterpart is that it offers a lower power consumption. However, it has a limited maximum input voltage and is more sensitive to changes of the supply voltage. On the other hand, shunt voltage references have no limit on the maximum input voltage, is not sensitive to change of the supply voltage and is able to create negative and floating reference voltages. Even though the shunt voltage reference has more advantages than the series, these advantages are not beneficial in this situation. Currently, Nuna uses a stable 5V voltage regulators and most series voltage references on the market have a maximum input voltage of up to 15 V. A negative and floating reference voltage is not needed, since a positive reference voltage does the same job in this situation. Therefore, the series voltage reference is the better topology, because of its lower power consumption.

Now that a topology has been chosen, a reference voltage has to be chosen. According to requirement [1.5] and [1.1], the output signal needs to be between 0V and 5V and the current range of -50A to 50A needs to be mapped into that voltage range. To have the same range of negative and positive currents, the reference voltage of 2.5V has been chosen.

3.7.1 Noise Analysis

The calculations of the noise voltage of the voltage reference can be done with equations 24 and 25. To calculate the noise voltage at the output of the system resulting from the voltage reference can be done with the same equation is for R_4 of the feedback network, equation 19. The noise voltage of several voltage references on the market are shown in figure 24 at bandwidths of 50 Hz and 100 Hz.

3.7.2 Component choice

In order to choose the best voltage reference, a few specifications need to be considered. The noise needs to be considered, because the SNR needs to be as high as possible at the output of the sensor system. The temperature coefficient needs to be as low as possible, since changes during operation resulted from temperature are not welcome. This can reduce the accuracy, below what is required. Figure 24 shows the comparison of the best voltage references on the market with its relevant parameters. Based on that, it is obvious that ADR4525B is the best voltage reference.

Product	1/f (µVpp)	Noise (nV/√Hz)	Total noise @100 Hz (µVrms)	Total noise @50 Hz (µVrms)	TC (ppm/C)	Offset @ 2.5 V [µV/C]
ADR441B	1.2	48	0.4973529934	0.3635381686	3	7.5
ADR4525B	1.25	41.3	0.4437509186	0.3341113254	2	5
ADR431B	3.5	80	0.9572239956	0.7721902471	3	7.5
MAX6525C_A	1.75	80	0.8130617716	0.5840115105	3	7.5
MAX873A	1.5	89	0.8805623203	0.615905837	1	2.5
LTC-6652AHMS8-2.5	3.8	216	2.144796287	1.505772596	7	17.5
ISL21007CFB825Z	5.25	238	2.421484049	1.741087304	5	12.5

Figure 24: Comparison of voltage references [23]

3.8 Filter

The total noise in the system is dependent on the noise bandwidth, see section 3.4. In order to reduce the noise the bandwidth should be limited. The total noise in the system should not exceed $5.2\mu V_{rms}$ to have an accuracy of $1mA$ (requirement [2.1]), see section 3.3.

To limit the bandwidth a first order low-pass filter will be used. The equivalent noise bandwidth (ENB) will be $1.57 * f_c$ (cut-off frequency) [13]. Figure 25 show the relation between the cut-off frequency and the total noise at the output of the sensor based on equation 7.

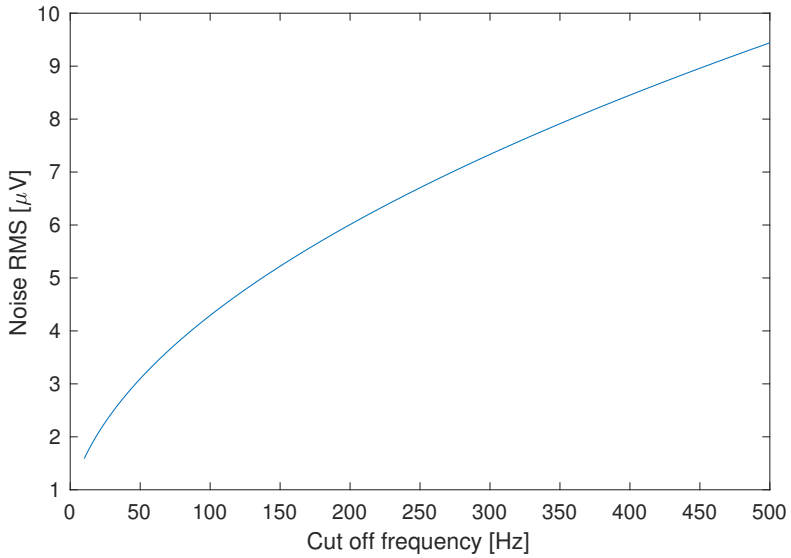

Figure 25: Cut off frequency of the filter versus total noise

Requirement [1.4] states that the communication frequency with the main computer of Nuna should be at least 5Hz. According to the Nyquist criterion the sample frequency should be at least twice the signal frequency. However the requirements states that a higher frequency is preferred. Looking to the noise the cut-off frequency is maximized at 150Hz.

An other aspect that must be kept in mind while choosing a cut-off frequency is the temperature drift of both the capacitor and the resistor. A change in temperature influences the capacitance and resistance and therefore possibly changes the cut-off frequency.

To implement the filter in the circuit a capacitor is added to the positive terminal of the differential amplifier and connected to the ground. To minimize the noise and keeping the temperature drift in mind a cut-off frequency of 127Hz will be implemented.

$$C = \frac{1}{2\pi f_c R}[F] \tag{27}$$

Using equation 27 with f_c = 1Hz and R = 500Ω results in a capacitance of $2.5\mu F$. Keeping the operating temperature of requirement of [1.3] in mind, the capacitance could change with $\pm 10\%$ [24]. The change in capacitance will result in a cut-off frequency between 115Hz and 141Hz which is beneath the maximum of 150Hz.

3.9 Error analysis

Every element in the sensor introduces errors in the output. The main errors are treated in the previous subsections. In this section the different errors will be summarized. The errors can be divided into standard errors and temperature drift errors.

3.9.1 Standard errors

The standard errors are calculated based on the maximum errors according to the data sheets [23, 25] and translated to the output with a gain of 50.

Source	**Type of error**	**Value**
Shunt resistor	Component tolerance	$\pm 125 \mu V/A$
Feedback network	Gain error due to component tolerances	$\pm 100 \mu V/A$
Amplifier (OPA189)	Voltage offset	$\pm 3 \mu V$
Amplifier	Input bias current	$\pm 0.06 \mu V$
Voltage reference (ADR4525B)	Offset error	$\pm 500 \mu V$

Table 3: Standard error

3.9.2 Temperature drift errors

The temperature drift errors are based on the maximum errors according to the data sheets [23, 25] and translated to the output with a gain of 50.

Source	**Type of error**	**Error per degree [°C]**	**Error at 60°C**
Shunt resistor	Component tolerance	$\pm 0.75 \mu V/A$	$\pm 26.25 \mu V/A$
Amplifier (OPA189)	Voltage offset	$\pm 1 \mu V$	$\pm 35 \mu V$
Amplifier	Input bias current	-	$\pm 0.2 \mu V$
Voltage reference (ADR4525B)	Offset error	$\pm 10 \mu V$	$\pm 350 \mu V$

Table 4: Temperature drift errors of the different sources

4 Testing

The goal of testing is not only to confirm that the system is working, but also to confirm that the components are working as the manufacturer has specified. Since noise is a very important aspect of the design of this sensor system, it would have been very valuable to be able to measure the noise of the system overall. Unfortunately, the equipment at the Tellegen Hall is not able to measure that, since the noise floor of oscilloscope was above the total noise of the system. Therefore, the only option is to rely on the noise analysis. Other important aspects that should be tested are the behaviour of the circuit when the temperature changes and when the input current changes.
Parameters that are important are the current of the current source and the output voltage of the amplifier, since it is crucial that the actual input current is the same as the display says it is.

4.1 Test setup

The test setup is made to replicate the proposed implementation of the sensor system. First, a current source is used to replicate the current that is coming from the batteries/MPPT/Motor. This current goes through the shunt resistor, which creates a small voltage. The voltage across the shunt resistor is amplified by the differential amplifier circuit. The differential amplifier is biased to 2.5 V by a voltage source. The amplifier uses voltage source that supplies 5 V. The current source and the 2.5 V reference voltage is supplied by a Tektronix PWS4205 Programmable DC Power Supply. In the test results the bias is subtracted. The input current and output voltage is measured with a Metrix mtx 3250. The Metrix mtx 3250 has a accuracy of $\pm 0.08\%$. With the Metrix mtx 3250 supply, the current was tested and adjusted to the correct value.

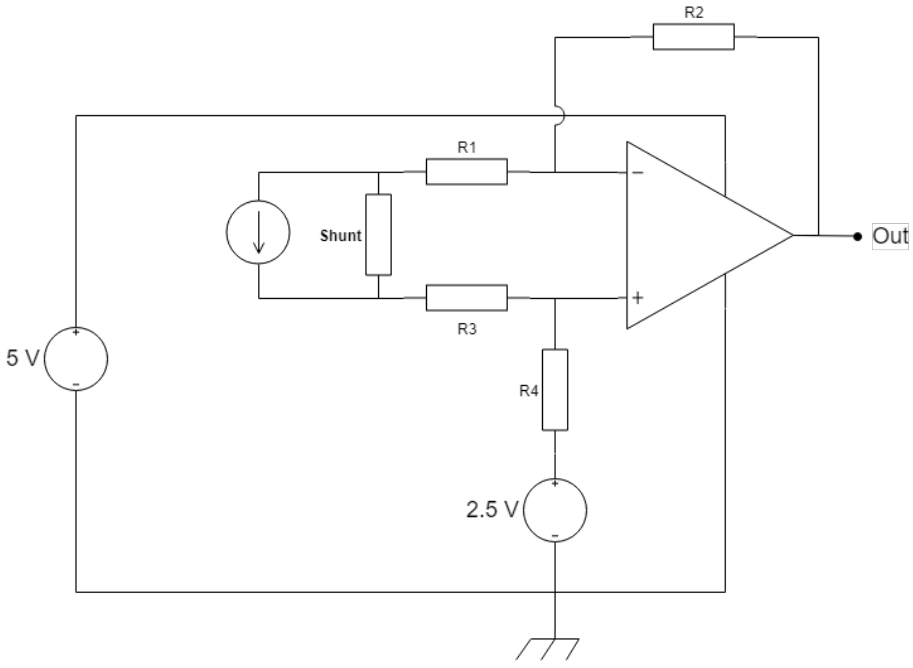

Figure 26: Test setup

4.2 Results

Figure 27 shows the measurements of the test with the OPA189 as amplifier. Figure 28 shows the corresponding error.

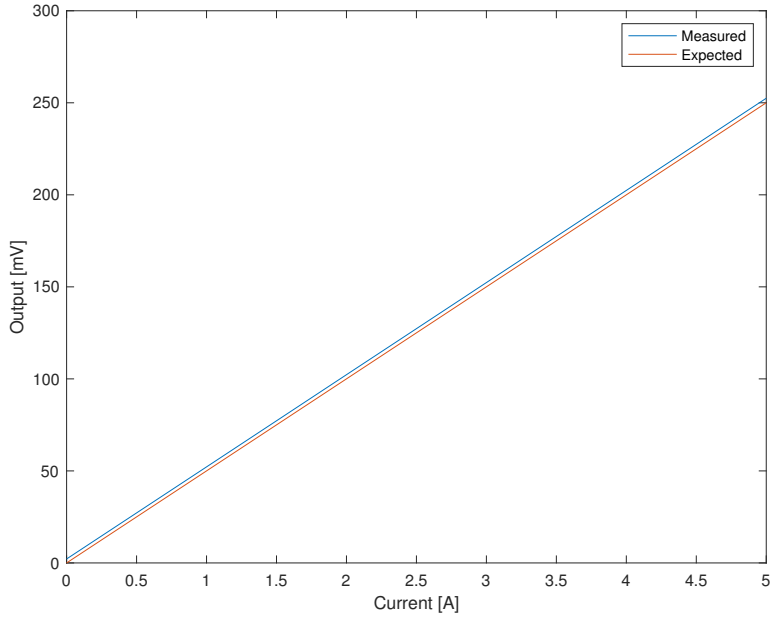

Figure 27: Test results

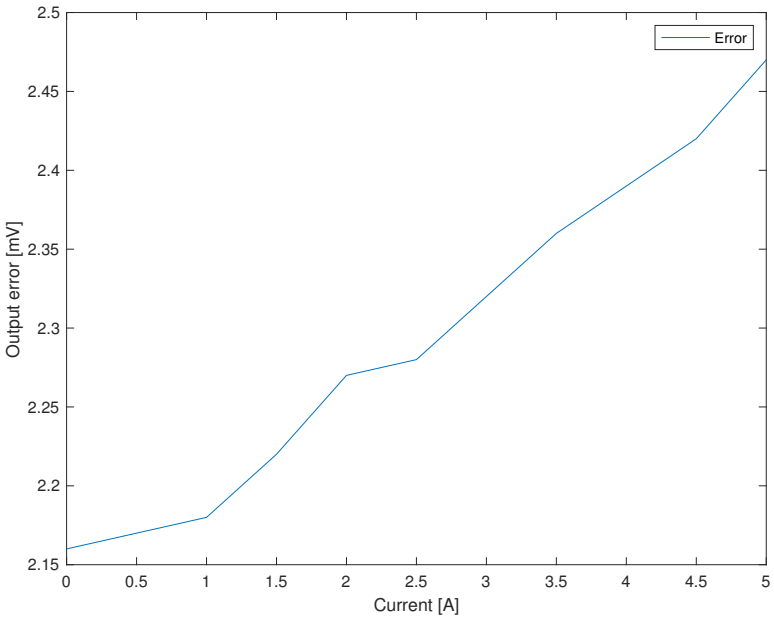

Figure 28: Error

5 Compensation

To fulfill requirements [1.1] and [1.3] the total errors caused by the elements in the circuit must be below 78 μV. To meet requirement [2.1] is must be below 31.2μV. Both the standard errors as well as the temperature depended errors need the compensated to reduce the errors. Compensation can be done using a software or a hardware solution [19].

5.1 Standard errors

The standard errors, summarized in section 3.9.1, can be divided into two categories. Errors dependent on the current and fully static errors.
The static errors could compensated by adding a voltage source at the output that opposes the total static errors. However, the error source could change over time [25] and components of the same type have a different error. Therefore it is more practical to compensate by software.
To calibrate the software a known current should be applied. The output voltage minus the expected output voltage should be subtracted of future measurements to compensate for the standard error.

The standard errors dependent on the current influence the transfer function of the circuit. The easiest way to compensate for these errors is to adjust the gain factor that the microprocessor uses to convert the output voltage of the sensor back to the current through the shunt resistor.

The gain of the circuit can be determined by applying two different currents at the input of the circuit and measuring the output voltage. The gain can be calculated using the following equation.

$$G = \frac{V_{out1} - V_{out2}}{I_1 - I_2} \tag{28}$$

5.2 Temperature dependent errors

The shunt resistor and the voltage reference cause the most dominant error. The other two errors can be neglected in order to meet requirement [1.1] and [1.3]. For both the shunt resistor as well as the voltage a software compensation is the most easiest solution. First the behaviour for the full temperature range should be analyzed. Based on this data a curve should be created.
A temperature sensor should be connected to the microprocessor. For the shunt resistor the gain factor must be adjusted based on the created curve and the temperature. For the voltage reference a compensation must be added to the output based on the created curve and the temperature.

6 Discussion

The noise calculations show that the noise is under the required noise mentioned in Chapter 3.3 to acquire the required SNR at the output of the operational amplifier. The total noise rms voltage graph can be seen in figure 25.
The voltage offset of $2.15mV$ in figure 28 is much higher than the expected voltage offset in table 3. However, this can be solved by calibrating.

Based on figure 28, there seems to be a gain error of the expected value, since the error is increasing as the current increases.
Nevertheless, the current sensor is able to measure changes of 1mA.

7 Conclusion

The sensor system needs a temperature compensation for the shunt resistor and the voltage reference. The voltage offset of the operational amplifier needs to be compensated. Both can be done either with software or hardware. However, software is the preferable option, since it is more precise than a hardware compensation.

The system needs to be tested with the addition of a low pass filter and a voltage reference IC. This has not been done yet due to time constraints caused by the realization that the old operational amplifier was too noisy for a 17 bits ADC. Moreover, there were some delivery problems of the voltage references, which made the group unable to test the system with voltage references.
Due to internal problems from the subgroup that is responsible for the ADC, the current sensor could not be tested together with the ADC.
Due to delay on the design of the current sensor, the voltage sensor has not been designed yet.

Bibliography

[1] Honour roll — world solar challenge 2019. [Online]. Available: https://www.worldsolarchallenge.org/about_wsc/history/honour_roll

[2] S. Ziegler, R. Woodward, and H. Iu, *Current sensing techniques: a review*. IEEE SENSORS JOURNAL, 2009.

[3] S. Ziegler, R. Woodward, H. Iu, and L. J. Borle, *Investigation Into Static and Dynamic Performance of the Copper Trace Current Sense Method*. IEEE SENSORS JOURNAL, 2009.

[4] E. Ramsden, *Hall-Effect Sensors: Theory and Application*. Elsevier, 2006.

[5] Q. Zhang, J. Liu, and Y. Yang, *A new complementary symmetrical structure of using dual magnetic cores for open loop Hall-Effect current sensors*. ?, 2015.

[6] S. J. Nibir, H. Niakan, and B. Parkhideh, "Characterization of magnetoresistors for contactless current sensing in power electronic applications," in *2017 IEEE Energy Conversion Congress and Exposition, ECCE 2017*, vol. 2017-January, 2017, pp. 433–438.

[7] J. Lenz and S. Edelstein, "Magnetic sensors and their applications," *IEEE Sensors Journal*, vol. 6, no. 3, pp. 631–649, 2006.

[8] H. G. Ramos and A. L. Ribeiro, "Present and future impact of magnetic sensors in NDE," in *Procedia Engineering*, vol. 86, 2014, pp. 406–419.

[9] J. Zubia, L. Casado, G. Aldabaldetreku, A. Montero, E. Zubia, and G. Durana, "Design and development of a low-cost optical current sensor." *Sensors (Basel, Switzerland)*, 2013.

[10] R. Wang, S. Xu, W. Li, and X. Wang, "Optical fiber current sensor research: review and outlook," *Optical and Quantum Electronics*, vol. 48, no. 9, 2016.

[11] B. Carter, P. Rowland, J. Karki, and P. Miller, "Amplifiers and bits: An introduction to selecting amplfiers for data converters," 1999.

[12] *Op Amp Noise Theory and Applications*, Texas Instruments, 2008.

[13] *Noise Analysis in Operational Amplifier Circuits*, Texas Instruments, 10 2007.

[14] T. Regan, J. Munson, G. Zimmer, and M. Stokowski, "Current sense circuit collection," 2015.

[15] K. Lokere, T. Hutchison, and G. Zimmer, "Precision matched resistors automatically improve differential amplifier cmrr - here's how," 2012.

[16] *DMS Accessories 50mV and 100mV Base-mounted DC Shunts*, muRata, 2015.

[17] P. Regtien, "Electronic instrumentation - operational amplifiers," vol. 2, pp. 182–197, 2015.

[18] R. Palmer, "Dc parameters: Input offset voltage," 2001.

[19] B. Nguyen and W. D. Smith, "Nulling input offset voltage of operational amplifiers," 2000.

[20] X. Zhang, "What you need to know about input bias current," 2016. [Online]. Available: https://e2e.ti.com/blogs_/b/analogwire/archive/2016/12/08/what-you-need-to-know-about-input-bias-current-and-why

[21] A. Sheikholeslami, "Chopper amplifier [circuit intuitions]," *IEEE Solid-State Circuits Magazine*, vol. 8, no. 2, pp. 7–9, Spring 2016.

[22] M. Edno, *Voltage Reference Selection Basics*, Texas Instruments, june 2014.

[23] *Ultralow Noise, High Accuracy Voltage References*, Analog Devices, 4 2012, rev. 0.

[24] *Chip Monolithic Ceramic Capacitor for General Electronic equipment GRM155C70J225ME11*, $muRata$, 2018.

[25] *OPAx189 Precision, Lowest-Noise 36-V, Zero-Drift, 14-MHz MUX-Friendly, Rail-to-Rail Output, Operational Amplifiers*, Texas Instruments, 11 2018, rev. A.